AMERICAN SOCIETY FOR MICROBIOLOGY | mBio®

RESEARCH ARTICLE
Molecular Biology and Physiology

Genome-Wide Characterization of the Fur Regulatory Network Reveals a Link between Catechol Degradation and Bacillibactin Metabolism in *Bacillus subtilis*

Hualiang Pi,[a] John D. Helmann[a]

[a]Department of Microbiology, Cornell University, Ithaca, New York, USA

ABSTRACT The ferric uptake regulator (Fur) is the global iron biosensor in many bacteria. Fur functions as an iron-dependent transcriptional repressor for most of its regulated genes. There are a few examples where holo-Fur activates transcription, either directly or indirectly. Recent studies suggest that apo-Fur might also act as a positive regulator and that, besides iron metabolism, the Fur regulon might encompass other biological processes such as DNA synthesis, energy metabolism, and biofilm formation. Here, we obtained a genomic view of the Fur regulatory network in *Bacillus subtilis* using chromatin immunoprecipitation sequencing (ChIP-seq). Besides the known Fur target sites, 70 putative DNA binding sites were identified, and the vast majority had higher occupancy under iron-sufficient conditions. Among the new sites detected, a Fur binding site in the promoter region of the *catDE* operon is of particular interest. This operon, encoding catechol 2,3-dioxygenase, is critical for catechol degradation and is under negative regulation of CatR and YodB. These three repressors (Fur, CatR, and YodB) function cooperatively to regulate the transcription of *catDE*, with Fur functioning as a sensor of iron limitation and CatR as the major sensor of catechol stress. Genetic analysis suggests that CatDE is involved in metabolism of the catecholate siderophore bacillibactin, particularly when bacillibactin is constitutively produced and accumulates intracellularly, potentially generating endogenous toxic catechol derivatives. This study documents a role for catechol degradation in bacillibactin metabolism and provides evidence that catechol 2,3-dioxygenase can detoxify endogenously produced catechol substrates in addition to its more widely studied role in biodegradation of environmental aromatic compounds and pollutants.

IMPORTANCE Many bacteria synthesize high-affinity iron chelators (siderophores). Siderophore-mediated iron acquisition is an efficient and widely utilized strategy for bacteria to meet their cellular iron requirements. One prominent class of siderophores uses catecholate groups to chelate iron. *B. subtilis* bacillibactin, structurally similar to enterobactin (made by enteric bacteria), is a triscatecholate siderophore that is hydrolyzed to monomeric units after import to release iron. However, the ultimate fates of these catechol compounds and their potential toxicities have not been defined previously. We performed genome-wide identification of Fur binding sites *in vivo* and uncovered a connection between catechol degradation and bacillibactin metabolism in *B. subtilis*. Besides its role in the detoxification of environmental catechols, the catechol 2,3-dioxygenase encoded by *catDE* also protects cells from intoxication by endogenous bacillibactin-derived catechol metabolites under iron-limited conditions. These findings shed light on the degradation pathway and precursor recycling of the catecholate siderophores.

KEYWORDS Fur regulon, ChIP-seq, catechol degradation, bacillibactin metabolism, bacillibactin degradation

Received 3 July 2018 **Accepted** 18 September 2018 **Published** 30 October 2018

Citation Pi H, Helmann JD. 2018. Genome-wide characterization of the Fur regulatory network reveals a link between catechol degradation and bacillibactin metabolism in *Bacillus subtilis*. mBio 9:e01451-18. https://doi.org/10.1128/mBio.01451-18.

Editor Arash Komeili, University of California, Berkeley

Address correspondence to John D. Helmann, jdh9@cornell.edu.

Iron is an essential micronutrient for most bacteria. It is required for many biological processes but can be toxic when present in excess. Various iron-mediated stress systems respond to changes in environmental iron availability (1, 2). Iron limitation induces acquisition systems to scavenge iron from the surroundings and activates systems to mobilize and prioritize iron utilization (3). Conversely, iron excess induces storage and efflux systems to maintain nontoxic levels of intracellular free labile iron (4, 5). These responses must be carefully coordinated by iron-responsive regulators to ensure effective iron balance within the cell. The ferric uptake regulator (Fur) is the key regulator of iron homeostasis in many bacteria (2). Fur monitors intracellular iron levels and regulates transcription of systems for iron uptake, utilization, storage, and efflux (6–8).

The Fur regulon has been characterized in many bacteria. In *B. subtilis*, the Fur regulon consists of an estimated 29 operons, many of which are involved in iron acquisition. These encode the biosynthesis machinery for the endogenous siderophore bacillibactin and uptake systems for elemental iron, ferric citrate, bacillibactin, and various xenosiderophores that are secreted by other microbes (8). In general, Fur functions as an iron-activated transcriptional repressor for most of its regulon. Under iron-replete conditions, Fur binds to its cofactor Fe^{2+}, and the resulting holo-Fur binds to its target sites and represses transcription of its target genes; when iron is limited, Fur loses its cofactor and apo-Fur dissociates from DNA, leading to derepression of its regulon. Recent results revealed that the Fur regulon is derepressed in three sequential waves (3). As cells transition from iron sufficiency to deficiency, *Bacillus* cells (i) increase their capacity for import of common forms of chelated iron that are already in their environment, such as elemental iron and ferric citrate, (ii) invest energy to synthesize their own siderophore bacillibactin and produce high-affinity siderophore-mediated import systems to scavenge iron, and (iii) express a small RNA FsrA and its partner proteins to prioritize iron utilization (3).

In addition to its regulatory role as a transcriptional repressor, holo-Fur can also activate gene expression, either directly or indirectly (5, 9, 10). For instance, in *Escherichia coli* Fur positively regulates expression of the iron storage gene *ftnA* by competing against the histone-like nucleoid structuring protein (H-NS) repressor when iron levels are elevated (5), and *Listeria monocytogenes* Fur activates the ferrous iron efflux transporter FrvA to protect cells from iron intoxication (9). Recent studies suggested that apo-Fur may act as a positive regulator in *E. coli* (11), and besides iron metabolism, the Fur regulon may expand into other biological processes such as DNA synthesis, energy metabolism, and biofilm formation (11–14). These findings motivated us to obtain a genomic view of the Fur regulatory network in response to iron availability in *B. subtilis*. Besides the known Fur target sites, 70 additional putative DNA binding sites were identified using chromatin immunoprecipitation coupled with high-throughput sequencing (ChIP-seq). Our attention was drawn to the binding site located in the promoter region of the *catDE* operon. This operon encodes a mononuclear iron enzyme, catechol 2,3-dioxygenase, which is critical for catechol degradation (15).

In this study, we demonstrated that holo-Fur functions as a repressor and works cooperatively with two other regulators, CatR and YodB, in regulating transcription of the *catDE* operon. This operon is induced upon catechol stress or iron limitation and is strongly induced when both conditions are present. Furthermore, accumulation of endogenous bacillibactin-derived catechol compounds triggers cell lysis, and CatDE is required to alleviate the toxicity. These findings suggest that CatDE is involved in metabolism of the triscatecholate siderophore bacillibactin and reveal a link between catechol degradation and bacillibactin metabolism in *B. subtilis*.

RESULTS AND DISCUSSION

Genome-wide identification of Fur binding sites by ChIP-seq. A recent study suggested that under anaerobic conditions *B. subtilis* Fur might regulate genes beyond its previously defined regulon (14). Moreover, our previous transcriptomic genome-wide studies of Fur regulation focused on those genes (as monitored by microarray

analysis) that were derepressed in both a *fur* mutant and in response to iron depletion. Since Fur might also act to activate gene expression, and some targets might not have been represented in the microarray (which was limited to annotated open reading frames [ORFs]), we chose to take an unbiased view toward defining those sites bound to Fur *in vivo* under both iron-replete and iron-deficient conditions using ChIP-seq. To modulate intracellular iron levels, we employed a high-affinity Fe^{2+} exporter, FrvA, from *L. monocytogenes* to impose iron starvation, as described previously (3, 9). *Bacillus* wild-type (WT) cells (with C-terminal FLAG-tagged Fur at their native loci and an isopropyl-β-D-thiogalactopyranoside [IPTG]-inducible ectopic copy of *frvA* integrated at their *amyE* loci) were harvested 0 and 30 min after IPTG induction to study Fur-dependent regulation under iron-sufficient and iron-deficient conditions, respectively (see details in "Materials and Methods").

Fur-dependent binding under iron-deficient conditions. ChIP-seq analysis identified 89 and 27 reproducible Fur binding sites (signal to noise ratio [S/N], ≥1.5) under iron-sufficient and iron-deficient conditions, respectively (Fig. 1 and Tables S3 and S4). Most of the binding sites (22 out of 27) occupied under iron-deficient conditions overlap those occupied under iron-sufficient conditions, so the total number of binding sites is 94 (Fig. 1B). Those sites occupied under both iron-sufficient and iron-deficient conditions may represent sites bound by holo-Fur that are of particularly high affinity and low dissociation rates or sites that can be occupied *in vivo* by apo-Fur.

Five ChIP peaks are specific to Fur under iron-deficient conditions and could represent authentic apo-Fur-specific sites (Fig. S1 and Table S4). One of these sites is located in the promoter of the *S477-ykoP* operon (Table S3), which encodes a possible regulatory RNA, S477, and a protein, YkoP, with unknown function. This operon has been implicated to be under negative regulation of multiple regulators, including Fur (8), ResD (14), NsrR (14), and Kre (16). A statistically significant ChIP peak (*P* value, ≥0.05) was detected in only one of the biological replicates (Table S3), indicating that the regulatory role of Fur at this site is uncertain. Four other apo-Fur-specific sites are located in intragenic regions, and Fur occupancy at these sites is fairly low (Fig. S1 and Table S4). The physiological significance of Fur binding at these sites is unclear. However, the ChIP peak located inside *ylpC* (also known as *fapR*) is very close to the 5′-end of the gene (Fig. S1D). FapR functions as a global regulator of fatty acid biosynthesis and is well conserved in Gram-positive bacteria (17). The *fapR* gene is under dual regulation: negative regulation by FapR itself (18) and positive regulation by the quorum sensing regulator ComA (19). Interestingly, transcriptome data show that expression of *fapR* is ~4-fold upregulated in a fur null mutant compared to WT (8), suggesting that *fapR* might be under negative regulation of Fur under iron-deficient conditions. Overall, our results suggest that apo-Fur has a limited role, if any, in gene regulation in *B. subtilis*. However, the connection between fatty acid biosynthesis and iron homeostasis deserves further investigation.

Known Fur target sites identified by ChIP-seq. Most of the previously defined Fur target sites (24 out of 27) were detected *in vivo* by ChIP-seq analysis (Fig. 1 and Table S3), which validated the modified method of ChIP-seq in *B. subtilis* (see details in "Materials and Methods") and further confirmed the Fur binding sites characterized by *in vitro* DNase I footprinting and transcriptome analysis (8). However, Fur occupancy at the promoter sites of *pfeT*, *yfkM*, and *ydhU/2-ydhU/1* was undetectable. The gene *pfeT* encodes an Fe^{2+}-efflux transporter, and its expression is activated by Fur only under excess iron conditions (20), which is likely why we were unable to detect Fur binding at this site under the conditions tested. The gene *yfkM* encodes a general stress protein that is under the regulation of SigB, and *ydhU2* and *ydhU/1* are two inactive pseudogenes. The previous study only detected very weak Fur binding at the promoter sites of *yfkM* and *ydhU/2-ydhU/1 in vitro*, and the Fur boxes identified at these two sites match only 10 out of 15 bases of the minimal 7-1-7 consensus sequence (8, 21). These results, together with the lack of measurable Fur occupancy *in vivo*, suggest that Fur may not play a significant role in the regulation of these genes.

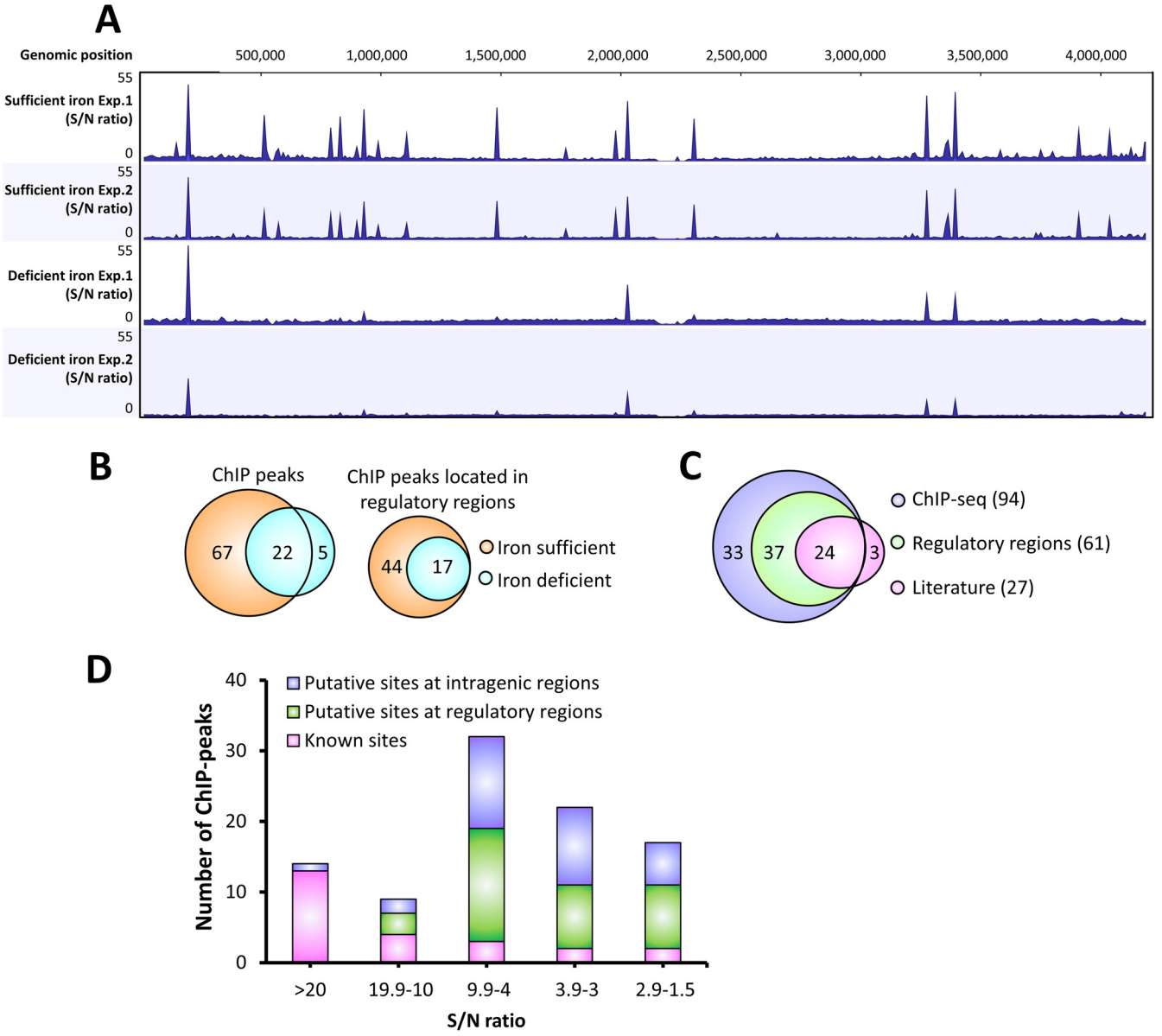

FIG 1 Overview of Fur-binding profiles across the *B. subtilis* genome under varied iron conditions. (A) ChIP-seq data of *B. subtilis* Fur-dependent binding under iron-sufficient and iron-deficient conditions. Most of the ChIP peaks showed higher occupancy under iron-sufficient conditions. Two biological replicates were included for each growth condition (Exp. 1 and Exp. 2). S/N denotes the signal-to-noise ratio for peak calling. (B) Most of the ChIP peaks (22 out of 27) identified under iron-deficient conditions overlap those detected under iron-sufficient conditions. The majority of peaks (61 out of 94) are located in regulatory regions. (C) Most of the known Fur binding sites from the literature (24 out of 27) are identified by ChIP-seq, with three exceptions (see the text). Among all the new identified Fur binding sites, 33 sites are located in intragenic regions, while 37 sites are located in regulatory regions. (D) Distribution of ChIP peaks relevant to the S/N ratio. The highest S/N ratio of each ChIP peak among all four samples was used for this analysis.

ChIP peaks located in intragenic regions. Many of the putative Fur binding sites identified by ChIP-seq (29 out of 70 sites) are located in intragenic regions (Table S4). Expression of most of these genes is not regulated by Fur (comparing mRNA levels between a *fur* mutant and WT) as monitored by microarray analysis (8) and quantitative PCR (qPCR) (Table S4 and S5), indicating an apparent lack of physiological relevance for these sites. We then evaluated the possible involvement of some putative targets under iron stress conditions (either iron intoxication or limitation). Among the five targets tested (the ones associated with high Fur occupancy, i.e., *ppsB*, *gidA*, *tufA*, *ybaC*, and *yycE*), none of the mutant strains showed sensitivity to high iron; only the *gidA* null mutant showed modest sensitivity to dipyridyl (an iron chelator that enters the cell cytosol and depletes intracellular iron pools) compared to WT (Table S5). The gene *gidA*

encodes a tRNA uridine 5-carboxymethylaminomethyl modification enzyme, and its role in iron homeostasis is currently under further investigation.

Another notable candidate for a functional intragenic Fur binding site resides within *ppsB*, the second gene in a long operon encoding a nonribosomal peptide synthetase (NRPS) that synthesizes the antibacterial compound plipastatin (a lipopeptide closely related to fengycins) (22). This peak has the highest Fur occupancy among all the newly identified sites (Table S4). Two divergently oriented promoters were assigned overlapping this ChIP peak (23), suggesting that transcription initiates internally to *ppsB*. In addition, a putative Fur box was identified within this peak area (11 out of 15 bases matching the consensus sequence) (Table S5). The transcriptome data showed that expression of *ppsB* is ~3-fold downregulated in a *fur* null mutant compared to WT (8), although this result was not confirmed by qPCR (Table S5). The *ppsB* null mutant showed no significant sensitivity to either iron intoxication or limitation compared to WT (Table S5). However, numerous studies document an important stimulatory role for iron in lipopeptide production in bacilli (24, 25), and lipopeptides can chelate metal ions (26) and likely iron. Together, these results lead us to speculate that transcripts encoded within *ppsB* may be regulated by Fur and perhaps function to coordinate plipastatin synthesis with iron status.

ChIP peaks located in regulatory regions. Among the 70 putative Fur target sites identified by ChIP-seq analysis, 37 are located in regulatory regions (Fig. 1C and D, Table S4). Most of these sites bind Fur under iron-sufficient conditions, although Fur also binds at some sites in at least one of the biological replicates under iron-deficient conditions (Table S4). At least 12 of these have good Fur boxes matching the minimal 7-1-7 consensus sequence (Table S5). Interestingly, Fur appears to bind to the promoter region of *gntR* in an iron-independent manner; Fur occupancy at this site remained at about the same level under both iron-deficient and iron-sufficient conditions (Table S4).

To evaluate the involvement of these putative Fur targets in iron homeostasis, we constructed deletion mutants of the top 12 candidates and carried out assays to test their sensitivity to high levels of iron and dipyridyl (Table S5). None of these strains showed significant sensitivity to high iron. Five of them showed moderate sensitivity to dipyridyl, including *cspB*, *yhcJ*, *catD*, *narJ*, and *yybN* (Table S5). Transcriptome data suggest that expression of *cspB*, *catD*, and *narJ* might be under the regulation of Fur (3). The expression of *catD* is upregulated (3.3-fold), whereas that of *cspB* (0.3) and *narJ* (0.2) is downregulated in a *fur* null mutant compared to the WT strain (Table S5). The regulatory role of Fur in *catD* and *narJ* was further confirmed by mRNA quantification using qPCR (Table S5). Here, the bicistronic operon *catDE* was subject to further investigation to elucidate its physiological role in iron homeostasis.

Fur binds to the regulatory site of the *catDE* operon under iron-sufficient conditions. A reproducible ChIP peak was identified in the promoter region of the *catDE* operon under iron-sufficient conditions. The signal-to-noise ratio for peak calling is relatively high in both independent replicates (10.1 for Exp. 1 and 14.1 for Exp. 2; Fig. 2 and Table S4), and the ChIP DNA enrichment at this site, compared to the input DNA control, is statistically significant (the *P* value is 3.5×10^{-24} for Exp. 1 and 1.2×10^{-44} for Exp. 2; Table S4). The *catDE* operon encodes a putative catechol 2,3-dioxygenase that requires Fe^{2+} as its cofactor (15). CatE showed 2,3-dioxygenase activity *in vitro* and is essential for viability in the presence of catechol (15, 27).

We tested the sensitivity of either single (*catD* or *catE*) or double (*catDE*) mutant strains to catechol toxicity using both disk diffusion and Bioscreen growth assays. Our results confirmed that they are both involved in catechol detoxification (Fig. S2). Both assays were performed in Belitsky minimal medium because we noticed that the catechol toxicity is significantly diminished in LB medium (Fig. S3). This may be due, at least in part, to the ability of Fe, Cu, Mn, and other divalent metal ions (which are relatively abundant in LB medium) to form metal-catechol complexes, which can decrease catechol toxicity (Fig. S4).

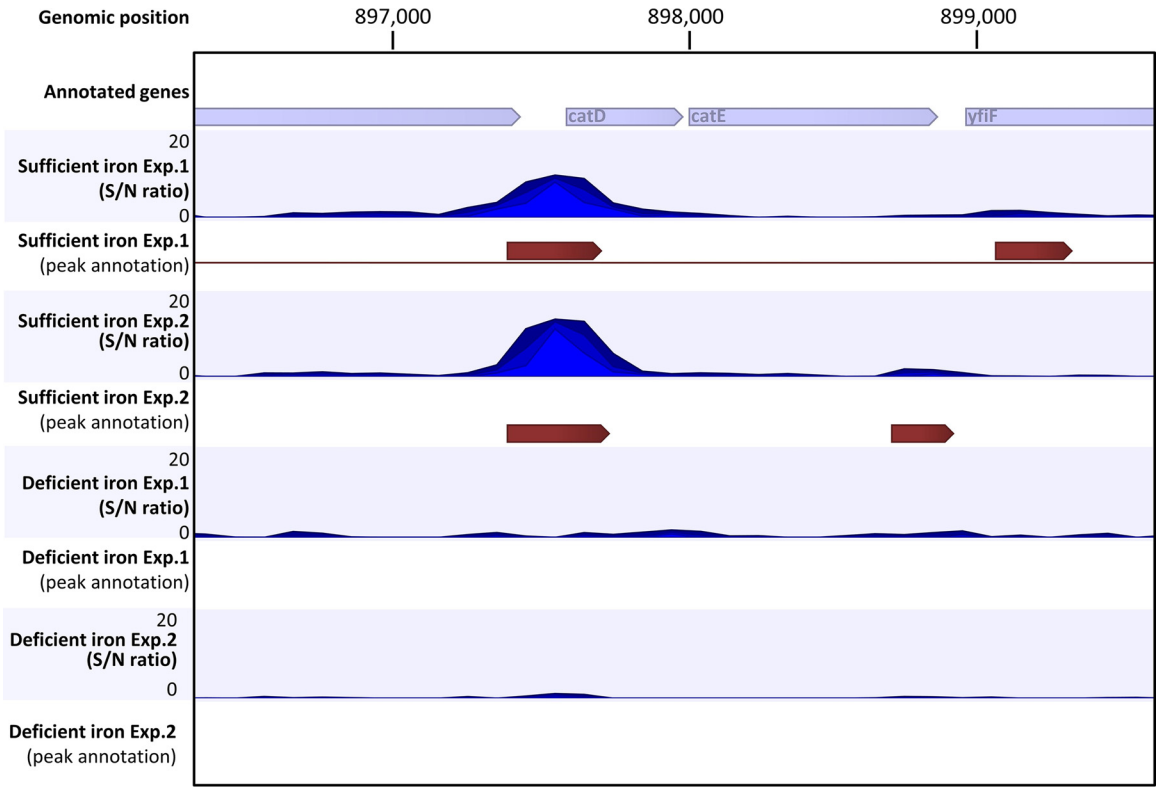

FIG 2 Fur binds to the promoter region of the *catDE* operon *in vivo* under iron-replete conditions. A zoom-in example of Fur binding at the *catDE* operon site identified by ChIP-seq. Two biological replicates were included as Exp. 1 and Exp. 2 for each condition. A single peak was annotated at this region for both replicates under iron-sufficient conditions. The peak length was 328 bp for Exp. 1 and 355 bp for Exp. 2. No peaks were annotated at this region for either replicate under iron-deficient conditions. S/N denotes the signal-to-noise ratio for peak calling.

Regulation of the *catDE* operon by three regulators. The *catDE* operon is under negative regulation of CatR, a MarR/DUF24 family transcription regulator that senses catechols, and YodB, a regulator of genes important for quinone and diamide detoxification (15). In addition, a Fur box (13 out of 15 bases match the minimal 7-1-7 consensus sequence [21]) is located downstream of the transcription start site (Fig. 3A), suggesting that Fur may act as a repressor. Indeed, qPCR measurements indicate that expression of *catD* was upregulated ~4-fold in the *fur* null mutant compared to WT cells (Fig. 3B), consistent with the previous transcriptome analysis (8).

We used electrophoretic mobility shift assays (EMSAs) to determine the affinity of Fur for the *catDE* operator site *in vitro*. Surprisingly, unlike the very high affinity (dissociation constant [K_d] of ~0.5 to 5.6 μM) observed with this same preparation of Fur protein for binding to most of its known target sites (3), the affinity of Fur for the *catDE* promoter is quite low (K_d of ~0.7 μM) (Fig. 4A and B). Fur binding to this site is specific (Fig. 4), and its binding affinity is comparable to that of either CatR or YodB binding to the same promoter region (15). Since all three regulators appear to bind rather weakly when tested individually, we suggest that these three regulators may interact with one another and bind to the promoter site cooperatively.

To dissect the cooperativity among the three regulators *in vivo*, a genetic study was performed using single, double, and triple deletion mutants of these three regulators, and *catD* mRNA levels were quantified under various conditions—iron sufficiency, iron limitation, and catechol stress. Consistent with the prior study (15), CatR functions as the major regulator and YodB plays a minor role in regulation of the *catDE* operon (Fig. 3B and C). When only one regulator is present (in the double mutants), YodB repression (in a *fur catR* double mutant) resulted in an ~4-fold reduction in mRNA compared to the full derepression observed in the triple mutant (*fur catR yodB*) (Fig. 3B

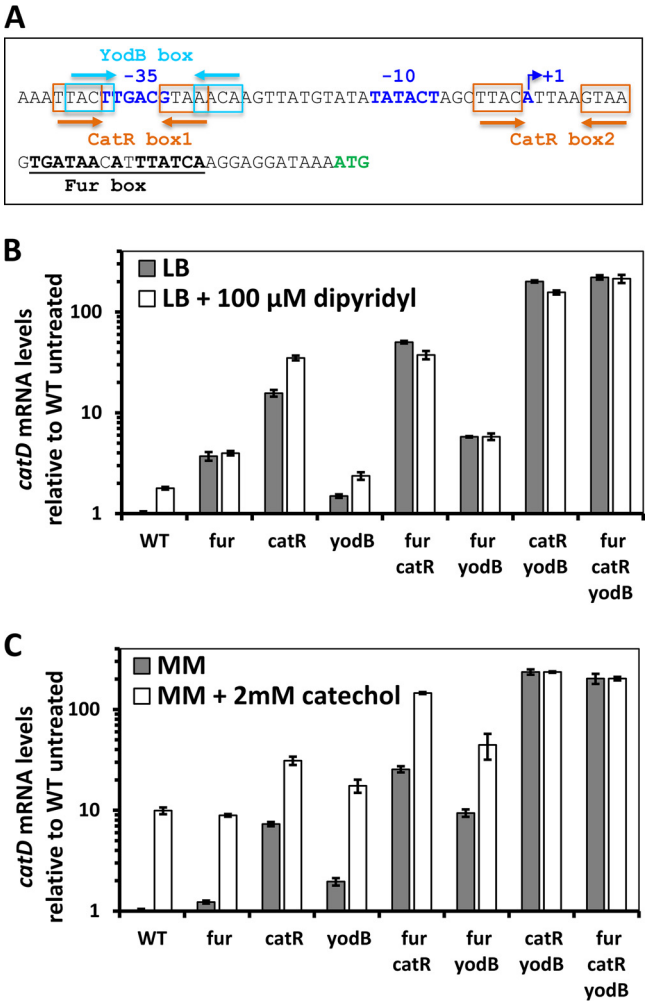

FIG 3 Regulation of the *catDE* operon by three transcription factors. (A) The promoter sequence of the *catDE* operon: −10, −35, and the transcriptional start site (+1) are highlighted in blue; the two CatR boxes are indicated by orange arrows; the YodB box is indicated by a light blue arrow; the Fur box is underlined. (B) The *catD* mRNA levels were compared among different strains grown in LB medium without or with 100 μM dipyridyl using qPCR. (C) The *catD* mRNA levels were compared among different strains grown in Belitsky minimal medium without or with 2 mM catechol using qPCR. The 23S rRNA gene was used as an internal control for both panels B and C.

and C). CatR is the major repressor and accounts for an ~38-fold reduction of *catD* expression (comparing the *fur yodB* double mutant to the *fur catR yodB* triple mutant). Interestingly, the *catD* mRNA level in the *catR yodB* double mutant is comparable to that in the triple mutant (Fig. 3B and C), indicating that Fur plays a negligible regulatory role when both CatR and YodB are absent, and Fur binding at this site *in vivo* may require, or be facilitated by, the other two regulators.

Either CatR or YodB facilitates Fur binding at the promoter site of *catDE*. To further explore whether CatR and/or YodB facilitate Fur binding *in vivo*, we evaluated Fur occupancy at the promoter site of *catDE* using ChIP-qPCR. No noticeable change of Fur occupancy was observed in the *catR* single mutant compared to WT cells, while Fur occupancy increased significantly in a *yodB* single mutant (Fig. 5A), indicating that Fur interacts with CatR more efficiently when YodB is absent, perhaps because YodB antagonizes CatR binding. This is consistent with the expression data, which showed that *catD* was induced by dipyridyl in the *catR* single mutant to a level comparable to that observed in the *fur catR* double mutant, whereas it was only partially derepressed by dipyridyl in the *yodB* single mutant compared to the *fur yodB* double mutant (Fig. 3B). Interestingly, Fur occupancy decreased significantly when both regulators

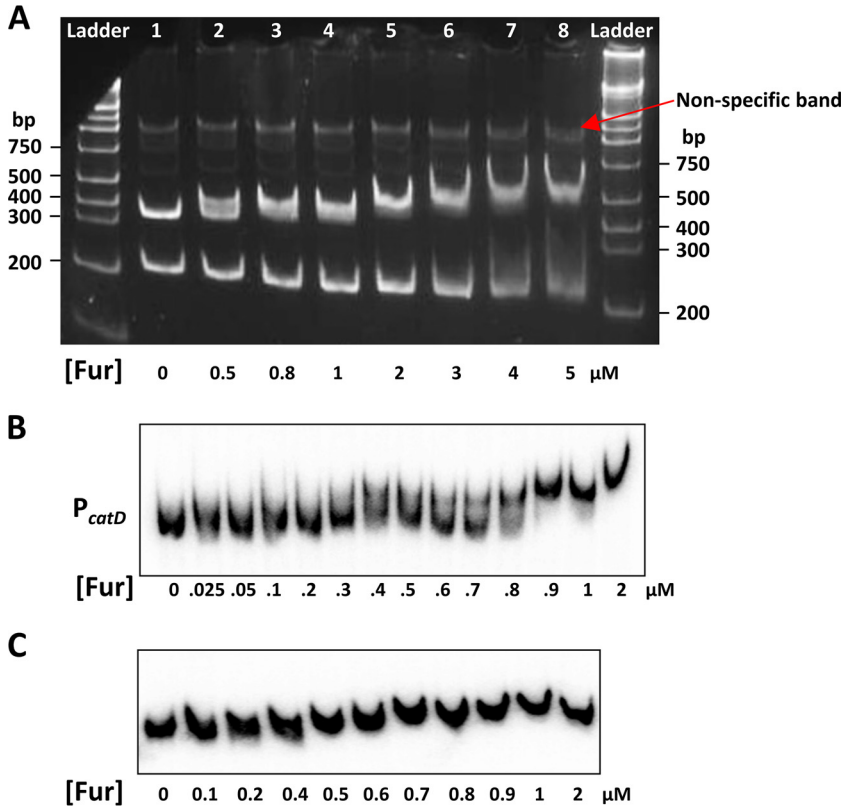

FIG 4 Fur specifically binds to the promoter region of *catDE in vitro*. An electrophoretic mobility shift assay (EMSA) was carried out using two sets of DNA probes. (A) The promoter region of *catD* and part of its open reading frame (–155 to +386 bp) were amplified by PCR and digested using HindIII, generating two fragments (lane 1): a 323-bp band (–155 to +168 bp; middle band) encompassing the promoter region and a 218-bp fragment located inside *catD* (+169 to +386 bp; bottom band), which serves as a negative control. A significant DNA shift (~50%) was observed with the lowest concentration of Fur (0.5 μM) for the middle band, whereas no evident DNA shift was observed with up to 3 μM of Fur protein for the bottom band. The red arrow indicates a nonspecific band from PCR amplification. About 180 ng of DNA probe was used for each reaction. The 5% native polyacrylamide gel was stained with ethidium bromide. (B) To determine the biochemical affinity of Fur binding to the operator site of the *catDE* operon, the promoter region (–121 to +76 bp) was PCR amplified and labeled at the 5′-ends with [γ-^{32}P]-ATP. The K_d value was calculated using GraphPad Prism 5 based on three independent experiments. (C) The DNA fragment (within the open reading frame of *catD*; +137 to +278 bp) was used as a negative control to evaluate nonspecific binding by Fur. No evident DNA shift was observed with up to 2 μM of Fur protein tested. Approximately 1 fmol of labeled DNA probe was used in each reaction shown in panels B and C.

were absent from the *catR yodB* double mutant (Fig. 5A). As expected, neither CatR nor YodB affected Fur occupancy at the promoter of *dhbA* (Fig. 5B). These results suggest that CatR and, to a lesser extent, YodB facilitate Fur binding at the promoter region of *catDE*. Similarly, NsrR and ResD have been reported to facilitate Fur binding at a minority of coregulated sites under anaerobic conditions; at most common sites, binding was competitive (14). At the apparently cooperative sites (*ykuN*, *fbpC*, and *exlX/yoaJ*), Fur appeared to facilitate binding of NsrR and/or ResD.

CatDE is involved in bacillibactin metabolism. The *B. subtilis* WT strain (168) and its derivatives do not normally synthesize bacillibactin, due to a null mutation in the *sfp* gene (*sfp*^{0}) encoding the phosphopantetheinyl transferase required for activation of the Dhb NRPS complex. Strains lacking functional Sfp secrete a mixture of 2,3-dihydroxybenzoate (DHBA) and its glycine conjugate (DHBG), collectively known as DHB(G). We used both an *sfp*^{0} strain and an isogenic strain with a corrected *sfp* gene (*sfp*$^+$) that produces bacillibactin for our iron homeostasis studies.

The expression of *catDE* is induced ~3-fold in both *sfp*^{0} and *sfp*$^+$ strains upon iron depletion imposed by dipyridyl (Fig. 3B and 6A and B), suggesting that CatD and/or

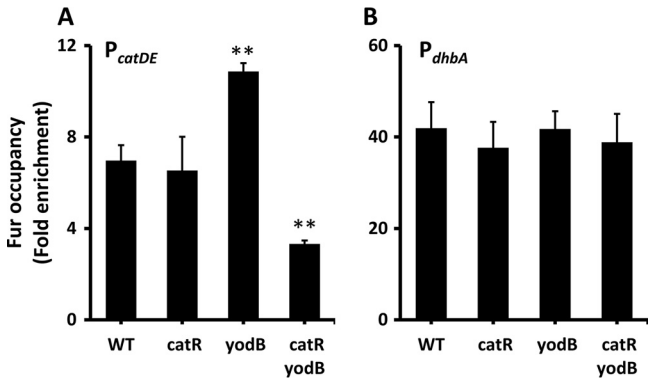

FIG 5 Either CatR or YodB facilitates Fur binding at the promoter site of *catDE*. Fur occupancy was evaluated by chromatin immunoprecipitation (ChIP) using anti-FLAG antibodies. Coimmunoprecipitated DNA was quantified by qPCR. DNA enrichment was calculated based on the input DNA (1% of total DNA used for each ChIP experiment). The data are presented as the fold enrichment of Fur occupancy at the promoter sites of *catDE* (A) and *dhbA* (B) (mean ± SD; $n = 3$). Significant differences between WT and mutant strains are indicated: **, $P < 0.01$. No significant DNA enrichment was observed for *gyrA*, which serves as a negative control.

CatE may be involved in iron homeostasis. To test this idea, the dipyridyl sensitivity of single (*catD* and *catE*) and double (*catDE*) mutant strains in both sfp^0 and sfp^+ backgrounds was evaluated using a disk diffusion assay. Indeed, both CatD and CatE play important roles in times of iron limitation since mutants were more strongly growth inhibited in the presence of the iron chelator dipyridyl (Fig. 6C and D). We therefore hypothesized that the enzymatic activity of CatDE may be required to detoxify bacillibactin-derived catechol compounds produced upon iron limitation. When iron is limited, bacillibactin is secreted into the environment to acquire iron, and the Fe^{3+}-bacillibactin complex is imported back into the cell through the FeuABC-YusV system. Iron is released and bacillibactin is cleaved into bacillibactin monomers (2,3-dihydroxybenzoate-gly-thr) and perhaps further processed into catechol derivatives, which may require CatDE for detoxification.

We employed a genetic approach to evaluate the involvement of CatDE in bacillibactin metabolism. We used a *fur ymfD* double mutant in which bacillibactin is constitutively produced and accumulates intracellularly due to the loss of the YmfD bacillibactin exporter. We then asked whether the *catDE* operon is important for growth under these conditions. No growth defects were noticeable in the *fur ymfD catDE* quadruple mutant compared to the *fur ymfD* double mutant in the first 6 h; however, dramatic cell lysis was observed in the quadruple mutant afterward, while the double mutant continued growing (Fig. 7A). We inferred that the *catDE* operon is critical for maintaining cell fitness when bacillibactin-derived catechol compounds accumulate intracellularly. Indeed, introduction of a *dhbA* null mutation to the quadruple mutant significantly rescued the cell lysis phenotype (Fig. 7A).

Once bacillibactin is imported back into the cytosol, it is hydrolyzed by the BesA esterase to release the chelated iron, and the siderophore is cleaved into three bacillibactin monomers. To understand whether the cell lysis defect is due to accumulation of bacillibactin or bacillibactin monomer, we introduced a *besA* null mutation to the quadruple mutant (*fur ymfD catDE*). In the absence of BesA, the cell lysis defect was no longer observed and cells grew almost as well as the *fur ymfD* double mutant (Fig. 7B). It is unknown whether or how bacillibactin monomers are further processed. Nevertheless, the bacillibactin monomer and perhaps derivative catechol compounds clearly require CatDE for detoxification.

Accumulation of intracellular bacillibactin-derived catechol induces *catD* expression. Since intracellular bacillibactin-derived catechol compounds can compromise cell fitness, we wished to determine if they might also serve as inducers of the *catDE* operon. To test this, we compared *catD* mRNA levels in the *fur ymfD* double

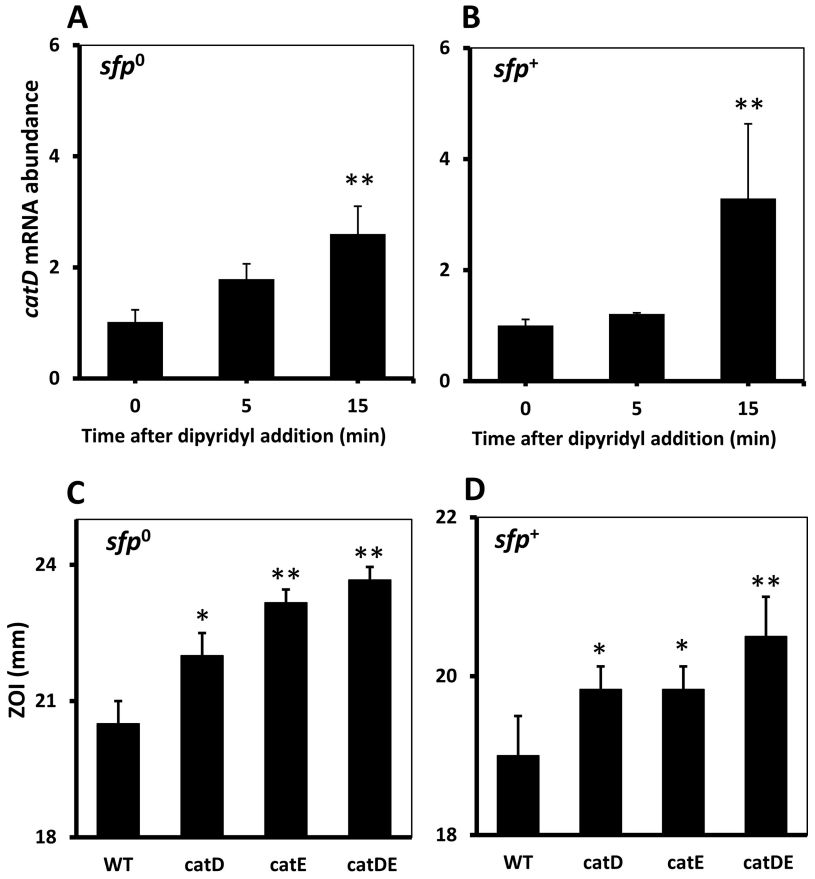

FIG 6 *catDE* is induced upon iron depletion and plays an important role in iron homeostasis. (A, B) Expression of *catD* was monitored in WT cells (A, *sfp*^{0}; B, *sfp*$^+$) grown in LB medium before (0 min) and after treatment of 100 μM dipyridyl. A significant difference between treated and untreated groups is indicated as **, $P < 0.01$. (C, D) Dipyridyl sensitivity of WT, single (*catD* and *catE*), and double (*catDE*) mutant strains in both *sfp*^{0} (C) and *sfp*$^+$ (D) backgrounds was evaluated using a disk diffusion assay. The data are expressed as the diameter (mean ± SEM; $n = 3$) of the inhibition zone (mm). Significant differences between WT and mutant strains are indicated: *, $P < 0.05$; **, $P < 0.01$.

mutant and the *fur* single mutant. Indeed, *catD* expression increased in the double mutant (defective for bacillibactin efflux) compared to the *fur* single mutant. This induction is specifically due to the accumulation of intracellular bacillibactin-derived catechols, since deletion of either *dhbA* or *besA* abolished induction. To understand which regulator is responsible for this induction, we monitored the *catD* mRNA levels in the *fur catR* and *fur yodB* double mutants. When both Fur and CatR were absent, induction was no longer evident (Fig. 8), suggesting that YodB does not respond to the accumulating catechols. In contrast, when both Fur and YodB were absent, a similar level of induction was observed (Fig. 8). These results suggest that intracellular accumulation of bacillibactin-derived catechol metabolites can lead to at least partial inactivation of the CatR repressor, thereby leading to induction of the *catDE* operon. Since Fur and CatR bind cooperatively *in vivo*, this system may be tuned to respond sensitively to the accumulation of catechol compounds (sensed by CatR) during times of iron starvation (sensed by Fur).

Fur occupancy on the *catDE* operator site. The Fur target genes are derepressed in three sequential waves upon iron depletion (3), which provides insights into the distinct roles of the Fur targets in iron metabolism. To understand the temporal gene expression of *catDE*, we monitored the Fur occupancy on this operator site using a chromosomal FLAG-tagged Fur in both WT and P_{spac}-*frvA*. Using ChIP-qPCR, we found that Fur dissociated rapidly from the DNA binding site, and an ~50% decrease in Fur occupancy was observed within 3 min upon FrvA induction (Fig. 9). We then compared

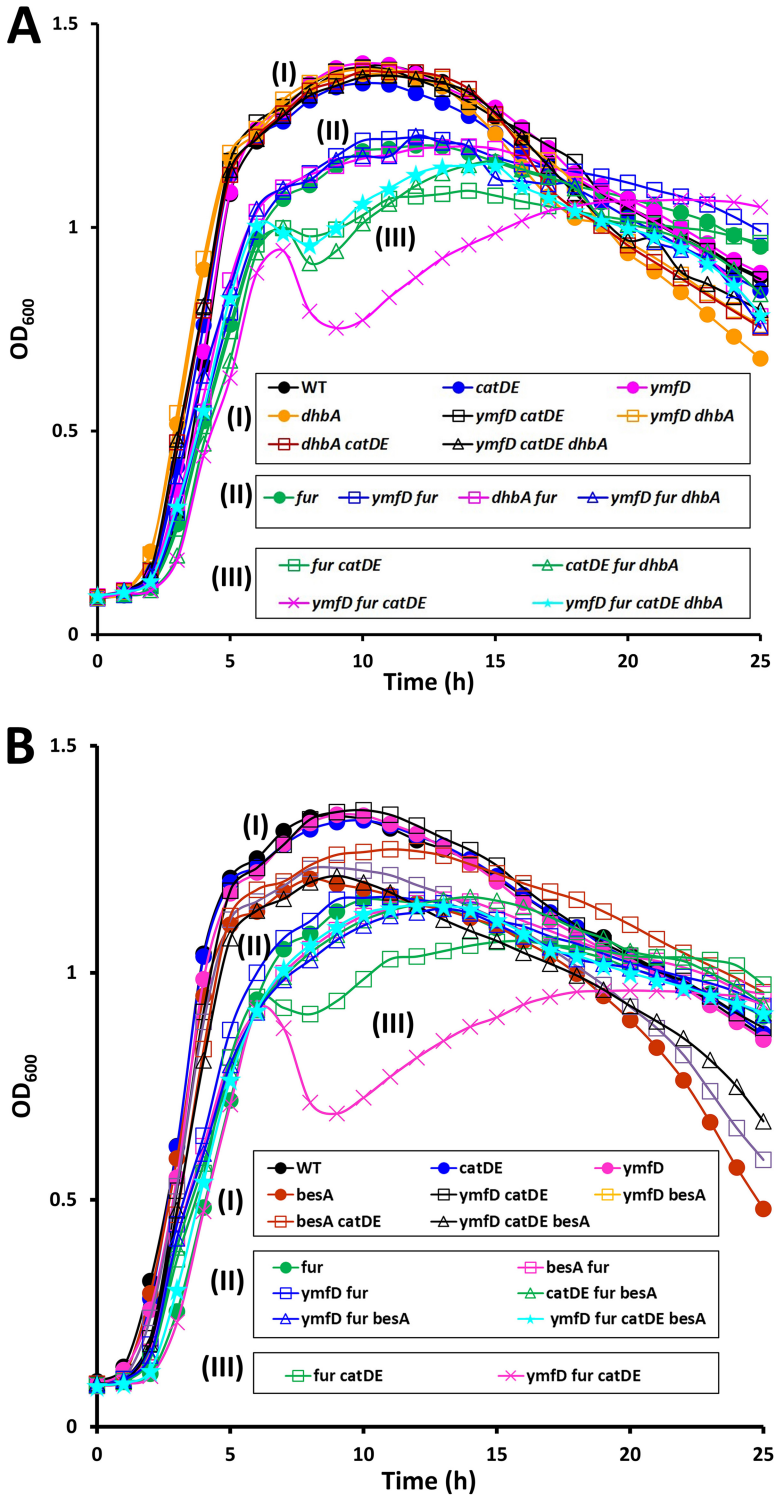

FIG 7 CatDE-mediated bacillibactin metabolism affects growth. (A, B) Representative growth curves are shown for strains that constitutively produce bacillibactin (*fur* mutation) and accumulate bacillibactin intracellularly (due to loss of the bacillibactin exporter YmfD). To check whether CatDE is required for bacillibactin metabolism, growth of WT (*sfp*$^+$) and its derived mutant strains was monitored in LB medium for 25 h. Experiments were performed three times with three biological replicates each time. The extent of lysis and the timing of regrowth were reproducible for the *fur ymfD catDE* mutant, suggesting adaptation in the surviving cells.

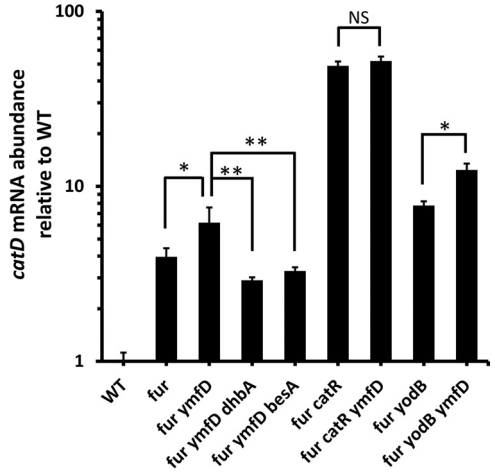

FIG 8 Accumulation of intracellular bacillibactin-derived catechol induces *catD* expression. The mRNA expression levels of *catD* were evaluated in WT (*sfp*$^+$) and its derived mutants grown in LB medium to an optical density at 600 nm of ~0.4. The 23S rRNA was used as an internal control. Significant differences are indicated as *, $P < 0.05$; **, $P < 0.01$. NS denotes not significant.

the Fur occupancy on this site with that on three Fur target sites that are representatives of the three sets of early, middle, and late genes determined previously (3). The results demonstrated that Fur occupancy on the *catDE* operator site followed the same pattern as that on the operator site of the late gene *fsrA* (Fig. 9), suggesting that *catDE* expression is induced after derepression of bacillibactin biosynthesis and bacillibactin-mediated uptake systems. We inferred that Fur derepression of *catDE* likely occurs soon after the onset of bacillibactin synthesis, and this leads to an initial modest increase in *catDE* expression that preemptively protects cells against the ensuing import of bacillibactin or other catecholate siderophores. In addition, because of the cooperative interaction of Fur and CatR *in vivo*, the loss of Fur repression also weakens the binding of CatR, thereby enabling a more sensitive derepression in response to accumulating catechols. Together, the loss of Fur and CatR repression enables the effective detoxification of siderophore-derived catechol compounds.

Concluding remarks. Here, we provide a global overview of potential targets of Fur-mediated gene regulation by mapping Fur binding sites under iron-replete condi-

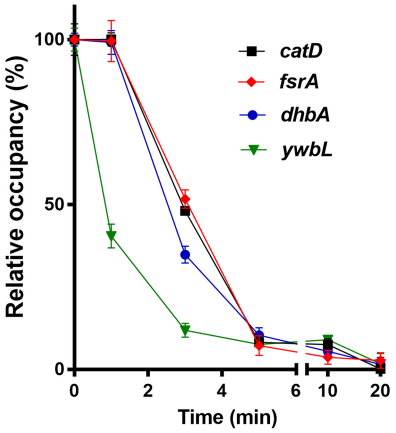

FIG 9 Fur occupancy on different operator sites. Fur occupancy was evaluated by ChIP-qPCR. DNA enrichment was calculated based on the input DNA (1% of total DNA used for each ChIP experiment). Fur occupancy at different sites was set as 100% at the zero time point. Dates are presented as the relative percentage (%) of occupancy at different time points after 1 mM IPTG induction of FrvA (mean ± SEM; $n = 3$). No significant DNA enrichment was observed for *gyrA*, which is used as a nonspecific negative control.

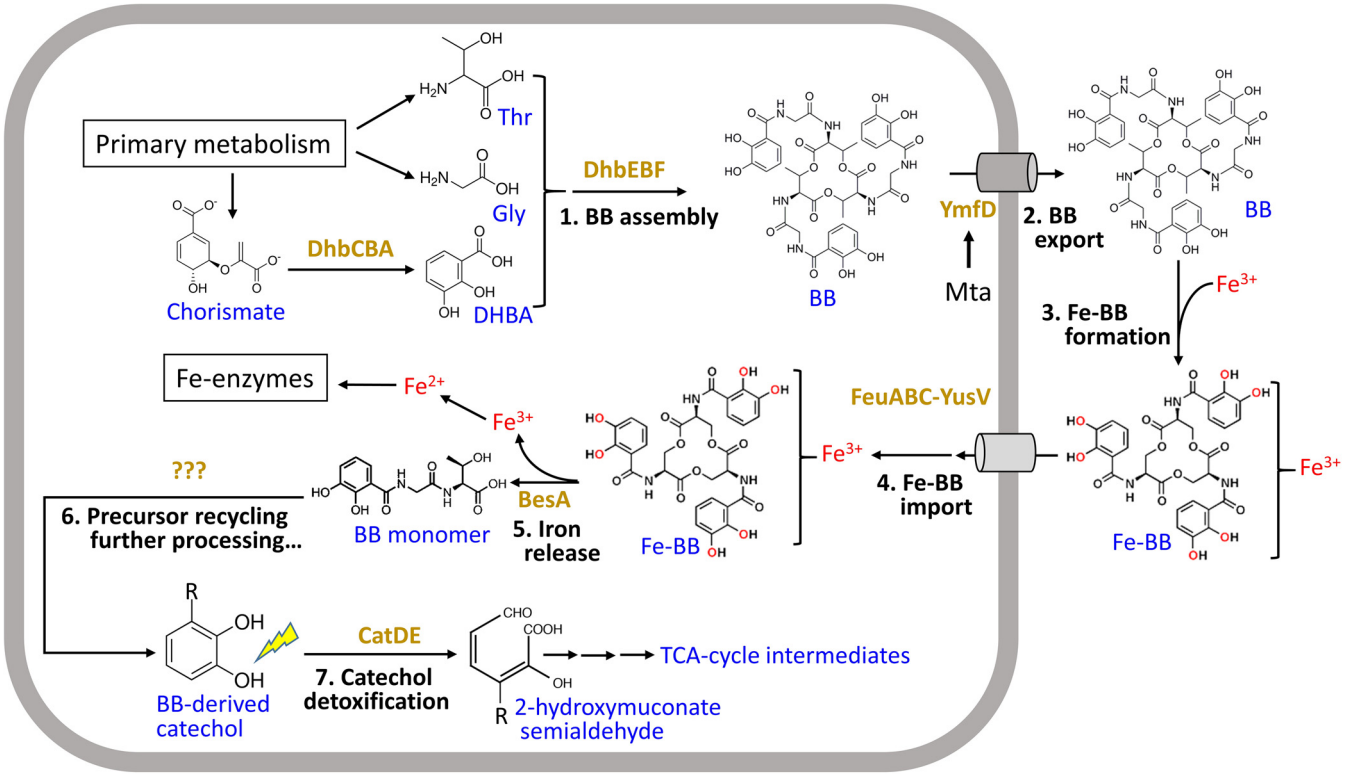

FIG 10 Role of catechol detoxification in bacillibactin metabolism. The endogenous siderophore bacillibactin (BB) is synthesized by an NRPS (nonribosomal peptide synthetase) assembly system (DhbACEBF) (28) and secreted by a major facilitator superfamily transporter YmfD, which is under regulation of the transcriptional activator Mta, a MerR family regulator of the multidrug-efflux transporter system (29). Bacillibactin chelates iron with very high affinity, and the resulting ferric-bacillibactin complex is then imported back into the cytosol through the FeuABC-YusV system and hydrolyzed by the BesA esterase to release iron (30), which yields three bacillibactin monomers (2,3-dihydroxybenzoate-Gly-Thr). It is still unknown whether or how the bacillibactin monomer is further processed. Nonetheless, it is clear that the bacillibactin monomer and perhaps bacillibactin-derived catechol compounds require CatDE for detoxification during metabolism.

tions and after the onset of iron deprivation. Our work confirms the core Fur regulon as defined previously (8) and suggests several new targets deserving of further study. These include potential roles for Fur in the regulation of the *S477-ykoP* and *pps* (plipastatin synthesis) operons and in the expression of FapR (a regulator of fatty acid synthesis), GidA (a tRNA modifying enzyme), CspB (cold shock protein), and NarJ (nitrate reductase). We focused our attention on the role of Fur in the regulation of *catDE*, encoding a catechol 2,3-dioxygenase.

Catechol 2,3-dioxygenase is an exceptionally well-studied enzyme notable for its central role in the biodegradation of a wide variety of aromatic compounds that generate catechol intermediates. Here, we provide a novel example of an endogenously produced intoxicant that relies on CatDE for its degradation (Fig. 10). After import of ferric-bacillibactin into the cytosol, the BesA esterase cleaves the triscatecholate siderophore to release iron, yielding three molecules of the bacillibactin monomer, 2,3-dihydroxybenzoate-Gly-Thr. In the absence of CatDE, this molecule, or its further degradation products, can be toxic and trigger cell lysis (Fig. 10). The expression of CatDE is under complex control involving three cooperatively functioning repressors. Binding of Fur to the *catDE* regulatory region appears to require cooperative interactions (largely with CatR). Upon the onset of iron deprivation, there is an initial modest induction of *catDE* (as inferred from the effect of a *fur* mutation) that preemptively synthesizes CatDE. As catechol compounds accumulate in the cell, due to import and processing of ferric bacillibactin or import of other catecholate xenosiderophores, inactivation of the CatR repressor leads to full induction. Since Fur and CatR bind cooperatively, once Fur is released, the CatR repressor binds more weakly, suggesting that the system is poised for a rapid response to catechol intoxication. To our knowledge, this is the first example of an endogenous intoxicant that is catabolized by CatDE. We also

present an example of a Fur target that is dependent on the cooperative action of multiple repressor proteins. This is reminiscent of the cooperative interactions documented previously for Fur, NsrR, and ResD reported for cells growing under anaerobic conditions (14).

MATERIALS AND METHODS

Bacterial strains and growth conditions. All strains used in the study are derivatives of *B. subtilis* CU1065 and are listed in Table S1. Cells were grown in LB or Belitsky minimal medium, and growth was monitored using a Bioscreen growth analyzer as described in Text S1.

RNA extraction and quantitative PCR (qPCR). Cells were grown at 37°C in LB medium, and RNA was purified for qPCR analysis as indicated in Text S1 using the indicated primers (Table S2).

Disk diffusion assay. Cells were grown in Belitsky minimal medium and assayed for sensitivity to 10 μl of 1 M catechol or 200 mM dipyridyl as described in Text S1. The data are expressed as the diameter of the inhibition zone (mm).

ChIP-seq, ChIP-qPCR, and data analysis. *B. subtilis* cells expressing a C-terminal FLAG-tagged Fur at the native locus and an ectopic copy of *frvA* integrated at the *amyE* locus were grown in LB medium amended with 25 μM iron to ensure Fur repression (3). 1 mM IPTG was added to induce expression of FrvA to deplete intracellular iron. ChIP was performed and analyzed by either Illumina-based sequencing (ChIP-seq) or qPCR (ChIP-qPCR) as described in detail in Text S1. Note that this ChIP-seq study was based on the same DNA analyzed previously using ChIP-qPCR, and negative controls using immunoprecipitated DNA from cells lacking Flag-tagged Fur were included in the earlier study (3).

Electrophoretic mobility shift assays (EMSAs). Binding of Fur (activated with 1 mM $MnCl_2$) to the *catD* promoter region was monitored using an EMSA. The K_d value, corresponding to the concentration of Fur that gives rise to 50% half-maximal shifting of the DNA probe, was evaluated and compared to *dhbA* as a positive control.

SUPPLEMENTAL MATERIAL

Supplemental material for this article may be found at https://doi.org/10.1128/mBio.01451-18.

TEXT S1, DOCX file, 0.03 MB.
FIG S1, DOCX file, 0.6 MB.
FIG S2, DOCX file, 0.2 MB.
FIG S3, DOCX file, 0.2 MB.
FIG S4, DOCX file, 0.5 MB.
TABLE S1, DOCX file, 0.03 MB.
TABLE S2, DOCX file, 0.01 MB.
TABLE S3, DOCX file, 0.03 MB.
TABLE S4, DOCX file, 0.04 MB.
TABLE S5, DOCX file, 0.03 MB.

ACKNOWLEDGMENTS

We thank members of the Helmann lab for helpful comments.

This work was supported by a grant from the National Institutes of Health to J.D.H. (R35GM122461).

H.P. and J.D.H. designed the research, H.P. performed the research, H.P. and J.D.H. analyzed the data, and H.P. and J.D.H. wrote the paper.

REFERENCES

1. Chandrangsu P, Rensing C, Helmann JD. 2017. Metal homeostasis and resistance in bacteria. Nat Rev Microbiol 15:338–350. https://doi.org/10.1038/nrmicro.2017.15.
2. Andrews SC, Robinson AK, Rodríguez-Quiñones F. 2003. Bacterial iron homeostasis. FEMS Microbiol Rev 27:215–237. https://doi.org/10.1016/S0168-6445(03)00055-X.
3. Pi H, Helmann JD. 2017. Sequential induction of Fur-regulated genes in response to iron limitation in *Bacillus subtilis*. Proc Natl Acad Sci U S A 114:12785–12790. https://doi.org/10.1073/pnas.1713008114.
4. Pi H, Helmann JD. 2017. Ferrous iron efflux systems in bacteria. Metallomics 9:840–851. https://doi.org/10.1039/C7MT00112F.
5. Nandal A, Huggins CC, Woodhall MR, McHugh J, Rodriguez-Quinones F, Quail MA, Guest JR, Andrews SC. 2010. Induction of the ferritin gene (*ftnA*) of *Escherichia coli* by Fe^{2+}-Fur is mediated by reversal of H-NS silencing and is RyhB independent. Mol Microbiol 75:637–657. https://doi.org/10.1111/j.1365-2958.2009.06977.x.
6. Ollinger J, Song KB, Antelmann H, Hecker M, Helmann JD. 2006. Role of the Fur regulon in iron transport in *Bacillus subtilis*. J Bacteriol 188:3664–3673. https://doi.org/10.1128/JB.188.10.3664-3673.2006.
7. Fleischhacker AS, Kiley PJ. 2011. Iron-containing transcription factors and their roles as sensors. Curr Opin Chem Biol 15:335–341. https://doi.org/10.1016/j.cbpa.2011.01.006.
8. Baichoo N, Wang T, Ye R, Helmann JD. 2002. Global analysis of the *Bacillus subtilis* Fur regulon and the iron starvation stimulon. Mol Microbiol 45:1613–1629. https://doi.org/10.1046/j.1365-2958.2002.03113.x.
9. Pi H, Patel SJ, Arguello JM, Helmann JD. 2016. The *Listeria monocytogenes* Fur-regulated virulence protein FrvA is an Fe(II) efflux P_{1B4}-type ATPase. Mol Microbiol 100:1066–1079. https://doi.org/10.1111/mmi.13368.
10. Delany I, Rappuoli R, Scarlato V. 2004. Fur functions as an activator and as a repressor of putative virulence genes in *Neisseria meningitidis*. Mol Microbiol 52:1081–1090. https://doi.org/10.1111/j.1365-2958.2004.04030.x.

11. Seo SW, Kim D, Latif H, O'Brien EJ, Szubin R, Palsson BO. 2014. Deciphering Fur transcriptional regulatory network highlights its complex role beyond iron metabolism in *Escherichia coli*. NatCommun 5:4910–4910.
12. Davies BW, Bogard RW, Mekalanos JJ. 2011. Mapping the regulon of *Vibrio cholerae* ferric uptake regulator expands its known network of gene regulation. Proc Natl Acad Sci U S A 108:12467–12472. https://doi.org/10.1073/pnas.1107894108.
13. Butcher BG, Bronstein PA, Myers CR, Stodghill PV, Bolton JJ, Markel EJ, Filiatrault MJ, Swingle B, Gaballa A, Helmann JD, Schneider DJ, Cartinhour SW. 2011. Characterization of the Fur regulon in *Pseudomonas syringae* pv. tomato DC3000. J Bacteriol 193:4598–4611. https://doi.org/10.1128/JB.00340-11.
14. Chumsakul O, Anantsri DP, Quirke T, Oshima T, Nakamura K, Ishikawa S, Nakano MM. 2017. Genome-wide analysis of ResD, NsrR, and Fur binding in *Bacillus subtilis* during anaerobic fermentative growth by *in vivo* footprinting. J Bacteriol 199:e00086-17. https://doi.org/10.1128/JB.00086-17.
15. Chi BK, Kobayashi K, Albrecht D, Hecker M, Antelmann H. 2010. The paralogous MarR/DUF24-family repressors YodB and CatR control expression of the catechol dioxygenase CatE in *Bacillus subtilis*. J Bacteriol 192:4571–4581. https://doi.org/10.1128/JB.00409-10.
16. Gamba P, Jonker MJ, Hamoen LW. 2015. A novel feedback loop that controls bimodal expression of genetic competence. PLoS Genet 11:e1005047. https://doi.org/10.1371/journal.pgen.1005047.
17. Albanesi D, de Mendoza D. 2016. FapR: from control of membrane lipid homeostasis to a biotechnological tool. Front Mol Biosci 3:64. https://doi.org/10.3389/fmolb.2016.00064.
18. Schujman GE, Paoletti L, Grossman AD, de Mendoza D. 2003. FapR, a bacterial transcription factor involved in global regulation of membrane lipid biosynthesis. Dev Cell 4:663–672. https://doi.org/10.1016/S1534-5807(03)00123-0.
19. Comella N, Grossman AD. 2005. Conservation of genes and processes controlled by the quorum response in bacteria: characterization of genes controlled by the quorum-sensing transcription factor ComA in *Bacillus subtilis*. Mol Microbiol 57:1159–1174. https://doi.org/10.1111/j.1365-2958.2005.04749.x.
20. Guan G, Pinochet-Barros A, Gaballa A, Patel SJ, Argüello JM, Helmann JD. 2015. PfeT, a P_{1B4}-type ATPase, effluxes ferrous iron and protects *Bacillus subtilis* against iron intoxication. Mol Microbiol 98:787–803. https://doi.org/10.1111/mmi.13158.
21. Baichoo N, Helmann JD. 2002. Recognition of DNA by Fur: a reinterpretation of the Fur box consensus sequence. J Bacteriol 184:5826–5832. https://doi.org/10.1128/JB.184.21.5826-5832.2002.
22. Tsuge K, Ano T, Hirai M, Nakamura Y, Shoda M. 1999. The genes *degQ*, *pps*, and *lpa*-8 (*sfp*) are responsible for conversion of *Bacillus subtilis* 168 to plipastatin production. Antimicrob Agents Chemother 43:2183–2192. https://doi.org/10.1128/AAC.43.9.2183.
23. Nicolas P, Mäder U, Dervyn E, Rochat T, Leduc A, Pigeonneau N, Bidnenko E, Marchadier E, Hoebeke M, Aymerich S, Becher D, Bisicchia P, Botella E, Delumeau O, Doherty G, Denham EL, Fogg MJ, Fromion V, Goelzer A, Hansen A, Härtig E, Harwood CR, Homuth G, Jarmer H, Jules M, Klipp E, Le Chat L, Lecointe F, Lewis P, Liebermeister W, March A, Mars RAT, Nannapaneni P, Noone D, Pohl S, Rinn B, Rügheimer F, Sappa PK, Samson F, Schaffer M, Schwikowski B, Steil L, Stülke J, Wiegert T, Devine KM, Wilkinson AJ, van Dijl JM, Hecker M, Völker U, Bessières P, Noirot P. 2012. Condition-dependent transcriptome reveals high-level regulatory architecture in *Bacillus subtilis*. Science 335:1103–1106. https://doi.org/10.1126/science.1206848.
24. Vivek R, Gunaseelan D, Ramya K, Ramkrishna S, Mahitosh M. 2012. Time-dependent dosing of Fe^{2+} for improved lipopeptide production by marine *Bacillus megaterium*. J Chem Technol Biotechnol 87:1661–1669.
25. Wei YH, Wang LF, Chang JS. 2004. Optimizing iron supplement strategies for enhanced surfactin production with *Bacillus subtilis*. Biotechnol Prog 20:979–983. https://doi.org/10.1021/bp030051a.
26. Mulligan CN, Yong RN, Gibbs BF, James S, Bennett HPJ. 1999. Metal removal from contaminated soil and sediments by the biosurfactant surfactin. Environ Sci Technol 33:3812–3820. https://doi.org/10.1021/es9813055.
27. Nguyen VD, Wolf C, Mader U, Lalk M, Langer P, Lindequist U, Hecker M, Antelmann H. 2007. Transcriptome and proteome analyses in response to 2-methylhydroquinone and 6-brom-2-vinyl-chroman-4-on reveal different degradation systems involved in the catabolism of aromatic compounds in *Bacillus subtilis*. Proteomics 7:1391–1408. https://doi.org/10.1002/pmic.200700008.
28. May JJ, Wendrich TM, Marahiel MA. 2001. The *dhb* operon of *Bacillus subtilis* encodes the biosynthetic template for the catecholic siderophore 2,3-dihydroxybenzoate-glycine-threonine trimeric ester bacillibactin. J Biol Chem 276:7209–7217. https://doi.org/10.1074/jbc.M009140200.
29. Miethke M, Schmidt S, Marahiel MA. 2008. The major facilitator superfamily-type transporter YmfE and the multidrug-efflux activator Mta mediate bacillibactin secretion in *Bacillus subtilis*. J Bacteriol 190:5143–5152. https://doi.org/10.1128/JB.00464-08.
30. Miethke M, Klotz O, Linne U, May JJ, Beckering CL, Marahiel MA. 2006. Ferri-bacillibactin uptake and hydrolysis in *Bacillus subtilis*. Mol Microbiol 61:1413–1427. https://doi.org/10.1111/j.1365-2958.2006.05321.x.